View metadata, citation and similar papers at core.ac.uk
brought to you by CORE
provided by The University of Utah: J. Willard Marriott Digital Library

Dissociative charge transfer reactions of Ar^+, Ne^+, and He^+ with CF_4 from thermal to 50 eV

Ellen R. Fisher, M. E. Weber,[a] and P. B. Armentrout[b]
Department of Chemistry, University of Utah, Salt Lake City, Utah 84112

(Received 28 August 1989; accepted 7 November 1989)

Guided ion-beam techniques are used to measure the cross sections for reaction of CF_4 with Ar^+, Ne^+, and He^+ from thermal to 50 eV. Dissociative charge transfer followed by successive loss of F atoms are the major processes observed. Only CF_x^+ ($x = 1$–3) products are observed in the reactions of Ar^+ and Ne^+. With He^+, in addition to the CF_x^+ products, both C^+ and F^+ are seen at high kinetic energies. Reaction rates for these reactions are also given and compared with previous measurements. It is found that the energy dependence of the cross sections can be understood by considering the energies needed to access specific electronic states of the CF_4^+ ion.

INTRODUCTION

Rare gases (Rg) are often an important component of plasmas used to etch and deposit silicon, silicon oxide, and silicon nitride layers. In plasma deposition processes, the starting material often consists of up to 90% rare gas diluents, in addition to the reactive gas. Although these diluents were initially believed to be inert, the amount and identity of the diluent has been found to significantly affect silane[1] and disilane[2] deposition characteristics. In the case of etching, energetic (1 keV) rare gas ions are often used in tandem with reactive neutral species, such as fluorides, to symbiotically enhance the etch rates and the directionality of the etched features.[3–5] The etch rate is highly dependent on the ion used (Ar^+, Ne^+, or He^+), yet the reasons for this dependency are unclear.[5] In other experimental plasma-etching systems, the substrates are immersed directly in the plasma either at ground or at the floating potential such that low-energy ions ($\leqslant 50$ eV) are incident on the substrates.[6]

Carbon tetrafluoride is used extensively in silicon etching plasmas as a source of reactive F atoms. In addition, CF_4/H_2 and CF_4/O_2 plasmas have been found to selectively etch both SiO_2 and Si_3N_4 surfaces in the presence of silicon surfaces.[7] Although the active etchant species in these plasmas are not known, it is likely that CF_3 and CF_2 radicals play an important role.[7] In addition, effective discharge conditions for these systems indicate that ion bombardment is required to initiate the selective etching.[8] Several possibilities exist for the mechanism responsible for ion-enhanced etching. The two primary mechanisms believed to be important are ion bombardment-induced gasification of the stable surface layer of fluorinated silicon formed when silicon is exposed to fluorine[8] and ion bombardment damage created in the near-surface region where impinging molecules react more rapidly at the damaged sites.[9] In addition to these mechanisms, ions also may promote chemical reactions involving other species, or may react directly with the substrate. With rare gas ions, dissociative charge transfer reactions could also be of importance since CF_3^+ and possibly CF_2^+ ions are likely to etch SiO_2 with significant probability.[10,11]

The study of rare gas ion–molecule reactions related to silicon etching and deposition plasmas containing CF_4 has been the focus of recent work. Cross sections for reaction of CF_4 with He^+ and Ne^+ have been measured at high energies (700–5000 eV).[12] Thermal reaction rates have been determined by using drift tube[13] and ion cyclotron resonance (ICR)[14] techniques. Also, UV emission from the $CF_4 + Rg^+$ interactions have been measured at collision energies of 1–1800 eV (Rg = Ar, Ne, He)[15] and 1–25 keV (Rg = He, Ne).[16]

Recent work in our laboratory has focused on ion–molecule reactions related to plasma systems involving SiF_4[17,18] and $SiCl_4$.[19] The mechanisms involved in the reactions of Si^+ with SiF_4 as well as the thermochemistry of the resulting SiF_x and SiF_x^+ species have been studied.[17] An analogous study was also performed with $SiCl_4$.[19] In addition, the reactions of rare gas ions with SiF_4 have also been explored.[18] The present work is a continuation of these studies.

EXPERIMENTAL SECTION

General

The ion-beam apparatus and experimental techniques used in this work are described in detail elsewhere.[20] The rare gas ions are produced as described below. The $^4He^+$, $^{22}Ne^+$, and $^{40}Ar^+$ ions are each mass analyzed and decelerated to the desired translational energy. The ion beam is injected into an rf octopole ion beam guide,[21] which passes through the reaction cell containing the CF_4 reactant gas. The CF_4 pressure is maintained sufficiently low, 0.01–0.1 mTorr, so that multiple ion–molecule collisons are improbable. The unreacted rare gas and product ions drift out of the gas chamber to the end of the octopole, where they are extracted and analyzed in a quadrupole mass filter. Ions are detected by a secondary electron scintillation ion counter using standard pulse counting techniques. Raw ion intensities are converted to absolute reaction cross sections as described previously.[20]

Laboratory ion energies (lab) are converted to energies in the center-of-mass frame (c.m.) by using the conversion $E(\text{c.m.}) = E(\text{lab})\cdot M/(m + M)$, where m is the ion mass and M is the CF_4 molecule mass.[20] This conversion factor is

[a] Present address: Texas Instruments, Dallas, TX 75265.
[b] NSF Presidential Young Investigator, 1984–1989; Alfred P. Sloan Fellow; Camille and Henry Dreyfus Teacher–Scholar, 1988–1993.

 © 1990 American Institute of Physics

Downloaded 11 Aug 2009 to 155.97.13.46. Redistribution subject to AIP license or copyright; see http://jcp.aip.org/jcp/copyright.jsp

0.96 for the He^+ reactions, 0.80 for the Ne^+ reactions, and 0.69 for the Ar^+ reactions. Unless stated otherwise, all energies quoted in this work correspond to the c. m. frame. The kinetic energy zero and the full width at half-maximum (FWHM) of the ion kinetic energy distribution are determined by using the octopole beam guide as a retarding potential analyzer.[20] The uncertainty in the absolute energy scale is ± 0.05 eV (lab). The distribution of ion energies have an average FWHM of 0.6 eV (lab) for He^+, 0.4 eV (lab) for Ne^+, and 0.3 eV (lab) for Ar^+.

Ion source

The rare gas ions are produced by electron impact of helium, neon, or argon gas, which have ionization potentials (I.P.) of 24.580, 21.559, and 15.755 eV, respectively.[22] The first excited electronic states of the ions are 65.4, 48.5, and 29.3 eV, respectively, above the neutral ground states.[22] Thus, to prevent formation of ionic excited states, the nominal electron energies used are 50, 35, and 20 eV, respectively. The electron energy distribution has a spread of less than $\pm$ 1.0 eV in each case. Only the $^2S_{1/2}$ ground state of He^+ is formed, but both the $^2P_{3/2}$ and $^2P_{1/2}$ spin–orbit states of Ne^+ and Ar^+ are produced, presumably with a 2:1 statistical population. The $^2P_{1/2}$ states of Ne^+ and Ar^+ lie 0.097 and 0.178 eV, respectively, above the $^2P_{3/2}$ ground states.[22] The $^{22}Ne^+$ isotope was used due to contamination by an impurity ion of mass 20 in the $^{20}Ne^+$ beam.

Ion collection efficiency

For charge transfer and dissociative charge transfer reactions, products may be formed through a long-range electron transfer such that little or no forward momentum is imparted to the ionic products.[23] In such instances, it is possible that up to 50% of these ions have no forward velocity in the laboratory and will not drift out of the octopole to the detector. Such slow product ions which do traverse the octopole may be inefficiently transmitted through the quadrupole mass filter.[20] Exothermic or nearly thermoneutral reaction channels, in particular, can be subject to these effects. Cross-section features and magnitudes for these channels were indeed found to be sensitive to the extraction and focusing conditions following the octopole. Results reported here were reproduced on several occasions and cross-section magnitudes shown are averaged results from all these data sets. Based on reproducibility, the uncertainty in the absolute cross sections is estimated as 40% in the Ne and Ar systems. The uncertainty for the He system is larger, 50–60%, due to difficulties associated with collecting low mass ions such as He^+. These problems have been discussed previously[24] and are minimized here by optimizing the collection and detection efficiency for low-mass products.

Thermochemical analysis

Exothermic reaction cross sections are usually described using the Langevin–Gioumousis–Stevensen (LGS) model[25]

$$\sigma_{LGS} = \pi e (2\alpha/E)^{1/2}, \qquad (1)$$

where e is the electron charge, α is the polarizability of the target molecule CF_4, and E is the relative kinetic energy of the reactants. Many exothermic reaction cross sections follow this type of energy dependence, although deviations from this behavior are commonly seen.[26] The polarizability of CF_4 is not well established. Calculated values for $\alpha(CF_4)$ extend from 2.38[27] to 3.91[28] Å^3, and experimental values range from 2.82[29]–2.92[30] Å^3. Here, we take the polarizability to be 2.92 Å^3.

At high kinetic energies, the collision cross section σ_{col} for charge transfer reactions may best be represented by the hard-sphere limit, given by

$$\sigma_{HS} = \pi R^2. \qquad (2)$$

R is roughly estimated by $r_e(Rg^+\text{–}F) + r_e(F_3C\text{–}F)$, where $r_e(F_3C\text{–}F) = 1.32$ Å.[31] For ArF^+, NeF^+, and HeF^+, the r_e values used here are 2.0, 1.56, and 1.33 Å, respectively.[32] This results in $\sigma_{HS}(Ar^+\text{–}CF_4) = 35$ Å^2, $\sigma_{HS}(Ne^+\text{–}CF_4) = 26$ Å^2, and $\sigma_{HS}(He^+\text{–}CF_4) = 22$ Å^2. In this work, σ_{col} is taken to be the maximum of σ_{LGS} and σ_{HS}.

Cross sections for endothermic reactions of species having a distribution of electronic states, denoted by i, can be analyzed by using

$$\sigma(E) = \sum_i g_i \sigma_{i0} (E - E_0 + E_i)^n / E^m, \qquad (3)$$

which involves an explicit sum of the contributions of individual states weighted by their populations g_i. Here, E_0 is the threshold for reaction of the lowest electronic level of the ion, E_i is the electronic excitation of each particular J level, σ_{i0} is an energy-independent scaling factor, and n and m are parameters which depend on the theoretical model being used. For the $J = 3/2$ and $J = 1/2$ spin–orbit states of the reactant ions Ar^+ and Ne^+, a 2:1 statistical population and equal reactivity are assumed, so that $g_{3/2} = 2/3$ and $g_{1/2} = 1/3$. Equation (3) has only a single term for He^+, since the $^2S_{1/2}$ state is the only electronic state of the ion formed.

In this study, Eq. (3) is evaluated for the cases where $m = 1$ for each endothermic reaction channel. The parameters n, σ_0, and E_0 are allowed to vary freely to best fit the data as determined by nonlinear least-squares analysis. This general form and its ability to reproduce the data has been discussed previously.[33] A value of $m = 1$ is chosen because this form of Eq. (3) has been derived as a model for translationally driven reactions[34] and has been found to be quite useful in describing the shapes of endothermic reaction cross sections and in deriving accurate thermochemistry from the threshold energies for a wide range of systems.[33,35] Errors in threshold values are determined by the variation in E_0 for the various models applied to several data sets.

RESULTS

For the reactions of rare gas ions with CF_4, there are three CF_x^+ product ions seen in all three systems, as given in

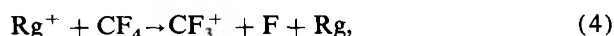

$$Rg^+ + CF_4 \rightarrow CF_3^+ + F + Rg, \qquad (4)$$

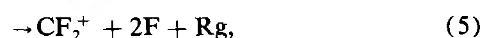

$$\rightarrow CF_2^+ + 2F + Rg, \qquad (5)$$

$$\rightarrow CF^+ + 3F + Rg. \qquad (6)$$

Formation of CF_4^+ and RgF^+ is not seen for any of the rare

Downloaded 11 Aug 2009 to 155.97.13.46. Redistribution subject to AIP license or copyright; see http://jcp.aip.org/jcp/copyright.jsp

gas ions studied here. In processes (5) and (6), fluorine can conceivably be liberated as either molecular fluorine or separated atoms. Although loss of F_2 is energetically favored over the loss of two F atoms (by 1.6 eV), the loss of F atoms is expected to be kinetically favored since it proceeds through a loose transition state and can more readily conserve angular momentum. Exclusive loss of F atoms was found in the similar $Rg^+ + SiF_4$ system.[18]

$Ar^+ + CF_4$

Results for the reaction of $Ar^+ + CF_4$ are shown in Fig. 1. At the lowest energies (below 0.1 eV), the total cross section declines as $(26 \pm 10)\ E^{-0.50 \pm 0.05}$. This behavior is in good agreement with the LGS model of Eq. (1) $\sigma_{LGS} = 29\ E^{-0.50}$. Between 0.1 and 2.5 eV, the cross section decreases more slowly as $E^{-0.3 \pm 0.04}$, and at a higher kinetic energies, the cross section levels off at about 34 $\text{Å}^2 \simeq \sigma_{HS}$. The observation that σ_{tot} is essentially equivalent to σ_{col} indicates that reaction occurs with 100% efficiency at all kinetic energies.

At all energies, formation of CF_3^+ [process (4)] is favored by at least an order of magnitude over other processes. At the lowest energies, the CF_3^+ cross section increases monotonically as the energy decreases, indicating an exothermic process. Indeed, the thermochemistry in Table I verifies that reaction (4) is exothermic by 1.07 ± 0.05 eV.

Reaction channels (5) and (6) are both highly endothermic processes. For CF_2^+ production, the apparent threshold is at ~ 6.0 eV. Analysis of this cross section using Eq. (3) leads to a reaction threshold of 6.55 ± 0.14 eV. These values are both well above the thermodynamic threshold for formation of $CF_2^+ + 2F$, 4.77 ± 0.13 eV (Table I). The CF^+ ion has an apparent threshold of ~ 10.5 eV, about 2.5 eV greater than the threshold for formation of $CF^+ + 3F$.

TABLE I. Heats of formation at 298 K (eV).[a]

Species	$\Delta_f H^0$	Species	$\Delta_f H^0$
C^+	18.754 (0.005)	F	0.823 (0.003)
C	7.428 (0.005)	F^+	18.311 (0.003)
CF^+	11.76 (0.09)[b]	He^+	24.652
CF	2.64 (0.09)[c]	$Ne^+(^2P_{3/2})$	21.638
CF_2^+	9.28 (0.13)[c]	$Ne^+(^2P_{1/2})$	21.735
CF_2	−2.12 (0.13)[c]	$Ar^+(^2P_{3/2})$	15.824
CF_3	−4.874 (0.0434)	$Ar^+(^2P_{1/2})$	16.001
CF_3^+	4.26 (0.043)[d]		
CF_4	−9.672 (0.0134)		

[a] Ion heats of formation are calculated using the convention that the electron is a monatomic gas. Values compared from the literature which use the "stationary electron" convention should be increased by 0.064 eV at 298 K. Unless otherwise noted, values are taken from M. W. Chase, Jr., C. A. Davies, J. R. Downey, Jr., D. J. Frurip, R. A. McDonald, and A. N. Syverud, *JANAF Thermochemical Tables*, 3rd ed. (AIP, New York, 1985); J. Phys. Chem. Ref. Data **14**, Suppl. 1, 1 (1985).

[b] J. M. Dyke, A. E. Lewis, and A. Morris, J. Chem. Phys. **80**, 1382 (1984).

[c] S. G. Lias, J. E. Bartmess, J. F. Liebman, J. L. Holmes, R. D. Levin, and W. G. Mallard, J. Phys. Chem. Ref. Data **17**, Supp. 1, 5 (1988).

[d] Recommended value from D. W. Berman, J. L. Beauchamp, and L. R. Thorne, Int. J. Mass Spectrom. Ion Phys. **39**, 47 (1981).

$Ne^+ + CF_4$

Figure 2 shows results for the reaction of Ne^+ with CF_4. Below about 1 eV, the total cross section is well below σ_{LGS}, reacting with only about 10–15% efficiency. At higher ener-

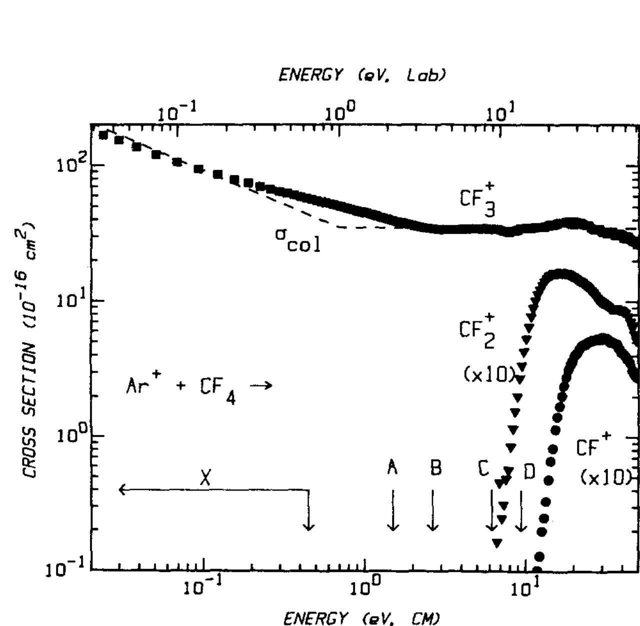

FIG. 1. The variation of product cross sections with translational energy in the laboratory frame of reference (upper scale) and the center-of-mass frame (lower scale) for the reaction of Ar^+ with CF_4. The dashed line shows the collision cross section, given by the maximum of either the hard sphere or LGS [$\alpha(CF_4) = 2.92\ \text{Å}^3$] cross sections [Eqs. (1) and (2)]. The arrows show the ΔI.P. values listed in Table III for the CF_4^+ states labeled.

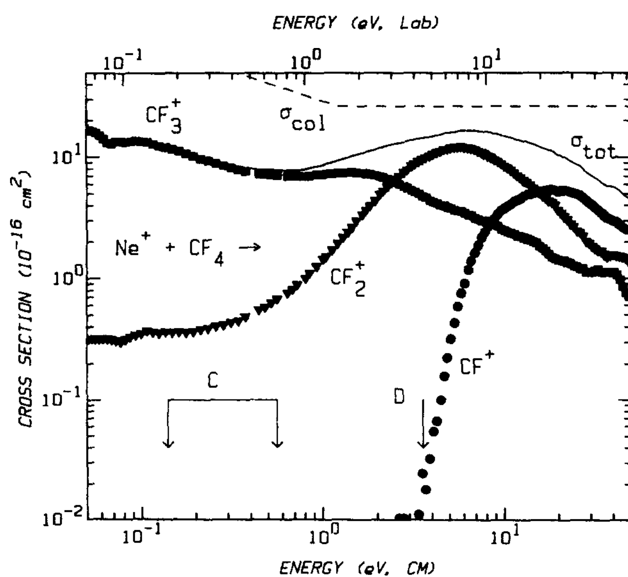

FIG. 2. The variation of product cross sections with translational energy in the laboratory frame of reference (upper scale) and the center-of-mass frame (lower scale) for the reaction of Ne^+ with CF_4. The solid line shows the total reaction cross section. The dashed line shows the collision cross section, given by the maximum of either the hard sphere or LGS [$\alpha(CF_4) = 2.92\ \text{Å}^3$] cross sections [Eqs. (1) and (2)]. The arrows show the ΔI.P. values listed in Table III for the CF_4^+ states labeled. For the C state, both the adiabatic and vertical values are shown.

Downloaded 11 Aug 2009 to 155.97.13.46. Redistribution subject to AIP license or copyright; see http://jcp.aip.org/jcp/copyright.jsp

gies, the maximum total cross section rises to about 65% σ_{col}, but then declines again.

The CF_3^+ product cross section shows exothermic behavior, increasing as the kinetic energy decreases. Although reaction (4) is exothermic by 6.88 ± 0.05 eV (Table I) this process is not very efficient even at the lowest energies (Fig. 2). At about 0.5 eV, a small second feature in the cross section begins, rises to a maximum of ~ 8 Å^2 at about 1.5 eV, and then decreases steadily thereafter. This decline is associated with a concomitant rise in the CF_2^+ cross section.

Process (5), the production of $CF_2^+ + 2F$, is exothermic by 1.04 ± 0.13 eV (Table I). The cross section for this process, however, does not increase monotonically with decreasing energy, as is typical for exothermic reactions. Above ~ 0.5 eV, the cross section for process (5) rises sharply and dominates the reactivity until about 12 eV. The CF_2^+ cross section declines significantly as process (6), the production of CF^+, becomes thermodynamically available, and at the highest energies, process (6) dominates the reactivity. Formation of CF^+ is endothermic, with an apparent threshold of ~ 3.5 eV. Analysis of this cross section using Eq. (3) yields a threshold of 4.03 ± 0.15 eV. Again, these values are higher than that calculated from Table I, 2.26 ± 0.09 eV.

The branching ratio between processes (4) and (5) in the Ne system is 96:4 at the lowest energies. As the kinetic energy increases, the branching ratio changes dramatically, with process (5) dominating over process (4), and by ~ 4.0 eV, the branching ratio between processes (4) and (5) has almost completely reversed to 20:80. Parker and El-Ashhab (PE) have measured the branching ratios for the $Rg^+ + CF_4$ systems at very high energies for Rg = Ne.[12] PE use 1000 eV Ne^+ ions and measure a product distribution of 32% CF_3^+, 25% CF_2^+, 17% CF^+, 14% F^+, and 12% C^+. We measure a product distribution between processes (4)–(6) at 50 eV of 53% CF_3^+, 32% CF_2^+, and 15% CF^+.

$He^+ + CF_4$

Reaction of He^+ with CF_4 (Fig. 3) is significantly different than those of Ar^+ and Ne^+. In addition to processes (4)–(6), formation of C^+ and F^+ are also seen at high kinetic energies. At all energies, the total cross section is well below the LGS prediction. Above 40 eV, the total cross-section magnitude levels off at nearly 60% of the collision limit.

Processes (4)–(6) are all exothermic based on Table I. At the lowest energies, the cross sections for processes (4) and (5) increase with decreasing energy, indicating exothermic processes, but these features decline at about $E^{-1.4 \pm 0.1}$. In addition, both cross sections have second features which begin between 2 and 4 eV. Formation of CF^+ [reaction (6)] is also exothermic (by 0.76 ± 0.09 eV, Table I), but, unlike processes (4) and (5), has only one feature[36,37] which is strongly endothermic. The apparent threshold is ~ 3.8 eV.

The final two reaction channels observed in the reaction of He^+ with CF_4 are formation of C^+ [process (7)] and formation of F^+ [process (8)]

$$He^+ + CF_4 \rightarrow C^+ + 4F + He, \quad (7)$$

$$He^+ + CF_4 \rightarrow F^+ + He + CF_{3-x} + xF (x = 0\text{–}3). \quad (8)$$

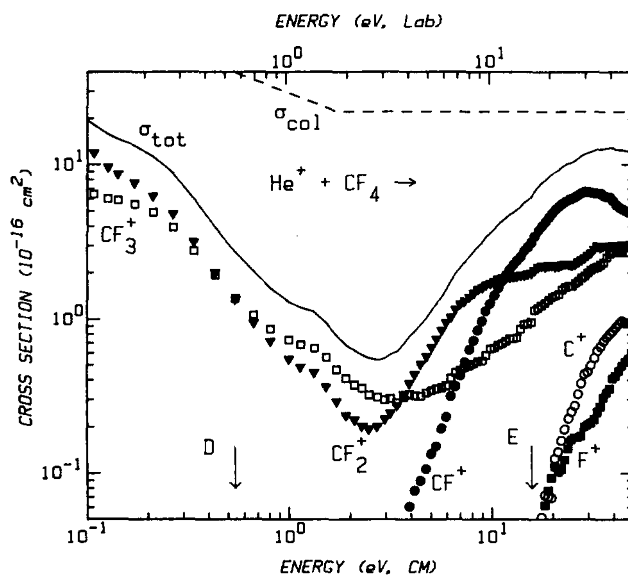

FIG. 3. The variation of product cross sections with translational energy in the laboratory frame of reference (upper scale) and the center-of-mass frame (lower scale) for the reaction of He^+ with CF_4. The solid line shows the total reaction cross section. The dashed line shows the collision cross section, given by the maximum of either the hard sphere or LGS [$\alpha(CF_4) = 2.92$ Å^3] cross sections [Eqs. (1) and (2)]. The arrows show the ΔI.P. values listed in Table III for the CF_4^+ states labeled.

Reaction (7) is endothermic by 7.1 ± 0.1 eV (Table I) well below the apparent threshold of ~ 15 eV. Reaction (8) is exothermic by 1.55 ± 0.05 eV for $x = 0$, and endothermic by 2.0 ± 0.1, 7.6 ± 0.1, and 13.22 ± 0.02 eV for $x = 1, 2$, and 3, respectively. The apparent threshold of ~ 11 eV indicates that the neutral fragments could include any of the fluorocarbon species CF, CF_2, or CF_3. The apparent threshold energy is too low, however, for complete atomization to be occurring.

The branching ratio between processes (4) and (5) in the He system is 35:65 at the lowest energies. This compares favorably with the measurement of 30:70 made by Richter and Lindinger (RL) at thermal energies.[13] From 0.4 to about 4.0 eV, the branching ratio rises from 50:50 to 60:40, where process (5) again dominates over process (4) at about 40:60 ± 10. In the He system, PE have also studied the reaction of $He^+ + CF_4$ at high kinetic energies. They use 900 eV He^+ ions and measure a product distribution of 54% CF_3^+, 24% CF_2^+, 10% CF^+, 5% F^+, and 4% C^+. At the highest energies studied here, 50 eV, we measure a distribution of 23% CF_3^+ 26% CF_2^+, 39% CF^+, 5% F^+, and 7% C^+. We speculate that PE observe less product dissociation than is seen here due to the configuration of their apparatus which discriminates against products formed with smaller impact parameters.

DISCUSSION

Reaction rates

Although kinetic rates for many reactions occurring in a plasma environment have been measured or estimated, the collection of kinetic data for these plasma systems is not complete. Figure 4 shows the total reaction rate constants as

Downloaded 11 Aug 2009 to 155.97.13.46. Redistribution subject to AIP license or copyright; see http://jcp.aip.org/jcp/copyright.jsp

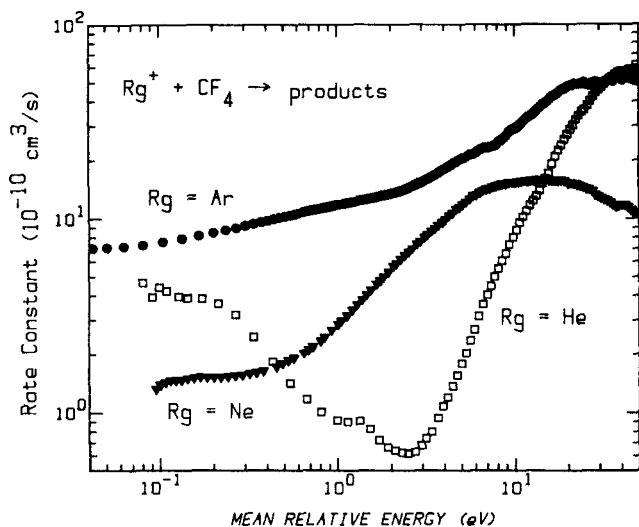

FIG. 4. Phenomenological rate constants for the reaction $Rg^+ + CF_4$ ($Rg = Ar$, Ne, and He) as a function of mean relative energy.

a function of energy for all three reaction systems.[38] For $Rg = Ar$ and Ne, the reaction rates are relatively constant at low energies, increase steadily as a function of energy, until they reach a maximum. The He system is markedly different. Although the reaction rate is fairly constant between 0.1 and ~0.2 eV, it *decreases* steadily between 0.2 and 3 eV. The reaction rate then rises sharply to a maximum of $\sim 60 \times 10^{-10}\ cm^3\ s^{-1}$.

Thermal reaction rate coefficients for the exothermic reactions measured here are given in Table II along with the LGS rate coefficients for the three rare gas systems. In the Ar system, the total rate for reaction is simply the rate for process (4), formation of CF_3^+, which proceeds at unit efficiency at all energies. Richter and Lindinger (RL) have used drift tube techniques to determine total reaction rates for the $Rg^+ + CF_4$ systems with $Rg = Ar$.[13] These thermal values are listed in Table II. For the Ar system, RL also observed that the rate coefficient for process (4) increases to $17.0 \pm 3.4 \times 10^{-10}\ cm^3\ s^{-1}$ at ~3 eV. For comparison, we measure a rate constant of $18.0 \pm 7.2 \times 10^{-10}\ cm^3\ s^{-1}$ at 3.0 eV. Thus, the rate constants measured here for the Ar system are in good agreement with those of RL. Using ICR techniques, Chau and Bowers (CB) have also measured the total reaction rates for the $Rg^+ + CF_4$ systems ($Rg = Ar$, Ne, and He), (Table II).[14] For the Ar system, our value is in good agreement with that measured by CB.

In the Ne system, both processes (4) and (5) contribute to the total reaction rate at thermal energies, which proceeds at only 14% of the LGS rate. For the Ne system, our total rate constant is again in good agreement with that derived by CB (Table II).

Much like the Ne system, both processes (4) and (5) contribute to the thermal rate constants in the He system. We take the near constant region between 0.1 and 0.2 eV to be representative of the thermal rate constant, and thus measure $4.0 \times 10^{-10}\ cm^3\ s^{-1}$. While somewhat higher than the values obtained by RL and CB (Table II), our value is within the combined uncertainties of these values. RL also measure a total reaction rate of $\sim 0.65 \times 10^{-10}\ cm^3\ s^{-1}$ at 0.36 eV. We measure a total rate constant for the He system of $2.2 \pm 1.1 \times 10^{-10}\ cm^3\ s^{-1}$ at 0.36 eV, again over twice the value of RL. While these values are within our generous error limits, the observed discrepancies could be explained by noting that the rate constant in the He system decreases rapidly as a function of energy below 2.0 eV. If the ion energies of RL and CB are somewhat higher than believed, this could cause their measured rates to be lower than the true thermal rate constants.

General behavior and realtive reactivity

The behavior displayed in the three Rg systems can be largely explained by examining the photoelectron spectrum (PES) of CF_4. Such spectra are available from a variety of sources.[39–41] Table III lists ionization energies for CF_4 from the UV PES of Brundle, Robin, and Basch (BRB)[39] and x-ray PES of Banna and Shirley.[40] Also listed are ΔI.P. values, the difference between the CF_4 ionization energies and the ionization potentials of the three rare gases.

In all three Rg systems, no CF_4^+ product is seen. This is similar to the observation that no parent ions have been observed by means of photon or electron impact mass spectrometry.[31,42] This is because the stable region of the CF_4^+ ground state is not accessible by a vertical transition from the CF_4 molecule. Rather, the region of the X state of CF_4^+

TABLE II. Thermal reaction rate constants.[a]

System	Product	Present work	RL[b]	CB[c]	LGS[d]
$Ar^+ + CF_4$	Total (CF_3^+)	7.0 (2.6)	8.0 (1.6)	6.4 (1.3)	7.6
$Ne^+ + CF_4$	CF_3^+	1.28 (0.26)			
	CF_2^+	0.06 (0.02)			
	Total	1.34 (0.40)		1.6 (0.3)	9.5
$He^+ + CF_4$	CF_3^+	1.4 (0.7)			
	CF_2^+	2.6 (1.3)			
	Total	4.0 (2.0)	1.8 (0.4)	2.7 (0.5)	20.5

[a] All rates in units of $10^{-10}\ cm^3\ s^{-1}$. Uncertainties are in parentheses.
[b] Richter and Lindinger (Ref. 13). Assumed 20% error.
[c] Chau and Bowers (Ref. 14).
[d] Langevin–Gioumousis–Stevensen collision rate $\alpha(CF_4) = 2.92$ Å^3.

Downloaded 11 Aug 2009 to 155.97.13.46. Redistribution subject to AIP license or copyright; see http://jcp.aip.org/jcp/copyright.jsp

TABLE III. Adiabatic and vertical ionization potentials for CF_4.[a]

Orbital	Adiabatic	Vertical	ΔI.P.(Ar)[b]	ΔI.P.(Ne)[b]	ΔI.P.(He)[b]
$X\,^2T_1$	⩾15.35	16.20	0.02(0.43)		
$A\,^2T_2$	17.10	17.40	1.50(0.15)		
$B\,^2E$	18.30	18.50	2.65(0.10)		
$C\,^2T_2$	21.70	22.12	6.16(0.21)	0.35(0.21)	
$D\,^2A_1$	25.12	25.12	9.37	3.56	0.54
$E\,^2T_2$	···	40.3[c]	24.55	18.74	15.72
$F\,^2A_1$	···	43.8[c]	28.05	22.24	19.22

[a] Except where noted, values are taken from Ref. 39.
[b] ΔI.P.(Rg) = I.P.(orbital)-I.P.(Rg) [Rg = Ar, Ne, or He] where I.P.(orbital) is the mean of the adiabatic and vertical values and the uncertainties (in parentheses) show the spread of these values.
[c] Values are from Ref. 40.

which is accessible via a vertical transition, as well as the lower lying A and B states of CF_4^+, all predissociate to $CF_3^+ + F$.[43] In addition, the C and D states of CF_4^+ are observed to radiate to the lower-lying states,[16,42] which then can dissociate.

Argon

The appearance of the $Ar^+ + CF_4$ reaction cross sections is nicely explained by referring to the PES of CF_4. The first PES band, the $X\,^1T_1$, occurs at ~15 eV, and peaks at about 16 eV (Table III). Argon ions (I.P. = 15.755 eV) are nearly resonant with this band (ΔI.P. ≈ 0 ± 0.4 eV), such that the reaction efficiency is high at all energies and favors CF_3^+. At higher kinetic energies, Ar^+ could produce the A and B states of CF_4^+, but these also form CF_3^+ exclusively (since formation of CF_2^+ requires more energy). Formation of the CF_2^+ product [reaction (5)] has an apparent threshold of ~6.0 eV (Fig. 1) corresponding directly to the ΔI.P. for the C band of CF_4^+ (Table III). Also the apparent threshold for reaction (6) occurs at ~10.0 eV, near the ΔI.P. for the D band of CF_4^+. Thus, the dissociative charge transfer reactions of argon ions with CF_4 are governed directly by the ability of the reaction system to access the various electronic states of the CF_4^+ ions. This leads to thresholds for fragmentation which are well above the thermodynamic values.

Neon

The same ideas can be applied to the Ne system. Here, charge transfer from Ne (I.P. = 21.56 eV) to produce the X, A, or B states of CF_4^+ are all exothermic processes. However, since none of these states are in resonance, Ne^+ does not react efficiently at low energies with CF_4. As the kinetic energy reaches the ΔI.P. value for the $C\,^2T_2$ band of CF_4^+, 0.35 ± 0.2 eV, (Table III), the cross section for process (5) and the total cross section increase noticeably (Fig. 2). Further, the ΔI.P. value for the D state of CF_4^+ corresponds nicely to the apparent threshold (~3.5 eV) for CF^+ formation, process (6) (Fig. 2). As in the Ar system, the reactivity of Ne^+ with CF_4 is correlated directly to the ability of the system to access higher electronic states of the CF_4^+ ion. This agrees with the conclusion of Parker and El-Ashhab[12] that $Ne^+ + CF_4$ charge transfer at elevated kinetic energies (1000 eV lab) populates the C state of the CF_4^+ which then predissociates.

Helium

As in the Ne system, helium ions (I.P. = 24.58 eV) are not resonant with any of the CF_4^+ states (Table III). This is consistent with the relative inefficiency of the reaction between He^+ and CF_4 at low energies (Fig. 3). The $D\,^2A_1$ band has a ΔI.P. value of 0.54 eV (Table III). This is somewhat below the second features in the CF_2^+ and CF_3^+ cross sections and the threshold for the CF^+ cross section, which do not begin until 2–3 eV. Further evidence that He^+ charge transfer leads to the D state of CF_4^+ at high kinetic energies (1000 eV lab) comes from the optical emission spectroscopy of Aarts, Mason and Tuckett.[42] Parker and El-Ashhab[12] have drawn a similar conclusion for 900 eV (lab) energy helium ions.

For the higher energy channels [reactions (7) and (8)], the apparent thresholds of ~15 and ~11 eV, respectively, do not correspond to any of the ΔI.P. values in Table III. However, the cross sections for these two reactions do not become appreciable until 15–17 eV, as can be seen in Fig. 3. This rise in the cross sections corresponds nicely to ΔI.P. for the E state of CF_4^+. Overall, the correlation between the onset of reaction cross section features and the PES bands of CF_4 is not as quantitative in the He system as it is in the Ar and Ne systems; however, there is a qualitative correspondence.

Relation to plasma systems

To predict the optimum physical parameters of a plasma system, it is first necessary to understand the interactions at the substrate and ascertain the primary chemical species responsible for the desired deposition or etching process. The gas-phase chemistry can then be tailored by modifying the starting materials and bias of the substrate to obtain the maximum concentration of reactive species.

CF_4 is used in plasma systems primarily as a source of the reactive F atoms. In addition, the CF_3^+ and CF_2^+ ions are of probable importance in the selective etching of SiO_2 and Si_3N_4 surfaces.[7] Mayer and Barker (MB) have also shown that the relative reactivities of the various CF_x^+ ions with SiO_2 are proportional to the number of F atoms in the

Downloaded 11 Aug 2009 to 155.97.13.46. Redistribution subject to AIP license or copyright; see http://jcp.aip.org/jcp/copyright.jsp

ion.[44] Thus, CF_3^+ and CF_2^+ ions contribute significantly more to the etching process than do CF^+ and C^+. This would suggest the use of Ar over Ne or He in the starting materials for etching of SiO_2 with CF_4 plasmas since the Ar system produces significantly more CF_3^+ than either the Ne or He systems.

As an additional comparison among the three systems, the reaction in the Ar system occurs with essentially unit efficiency at all energies, whereas in the Ne system, the maximum efficiency is only about 65% of σ_{HS} at about 8 eV, decreasing at higher energies. Although reaction efficiency does reach about 60% of σ_{HS} in the He system, it does so only at the highest energies (above 40 eV). Thus, the bias energy of the substrate in the plasma system can greatly affect the efficiency of reaction between the rare gas ions and CF_4.

ACKNOWLEDGMENT

This work was supported by the Air Force Wright Aeronautical Laboratories.

[1]J. C. Knights, R. A. Lujan, M. P. Rosenblum, R. A. Street, D. K. Biegle-sen, and J. A. Reimer, Appl. Phys. Lett. **38**, 331 (1981).
[2]T. L. Chu, S. S. Chu, S. T. Ang, A. Duong, Y. X. Han, and Y. H. Liu, J. Appl. Phys. **60**, 4268 (1986).
[3]J. W. Coburn and H. F. Winters, J. Appl. Phys. **50**, 3189 (1979).
[4]Y. Tu, T. J. Chuang, and H. F. Winters, Phys. Rev. B **23**, 823 (1980).
[5]U. Gerlach-Meyer, J. W. Coburn, and E. Kay, Surf. Sci. **103**, 177 (1981).
[6]J. W. Coburn, H. F. Winters, and T. J. Chuang, J. Appl. Phys. **48**, 3532 (1977).
[7]J. A. Mucha and D. W. Hess, Am. Chem. Soc. Symp. **219**, 215 (1983).
[8]J. W. Coburn, Plasma Chem. Plasma Proc. **2**, 1 (1982).
[9]V. M. Donnelly and D. L. Flamm, Solid State Technol. **24**, 261 (1981).
[10]J. L. Mauer and J. S. Logan, J. Vac. Sci. Technol. **16**, 404 (1979).
[11]S. C. McNevin and G. E. Becker, J. Vac. Sci. Technol. B **2**, 27 (1984).
[12]J. E. Parker and F. S. M. El-Ashhab, Int. J. Mass Spectrom. Ion Phys. **47**, 159 (1983).
[13]R. Richter and W. Lindinger, in *Proceedings of the Fourth International Symposium of Atomic Surface Physics*, edited by F. Howorka, W. Lindinger, and T. D. Mark (Inst. Atomphysik, Innsbruck, 1986), p. 202.
[14]M. Chau and M. T. Bowers, Int. J. Mass Spectrom. Ion Phys. **24**, 191 (1977).
[15]J. Sasaki, I. Kuen, and F. Howorka, J. Chem. Phys. **86**, 1938 (1987).
[16]J. F. M. Aarts, Chem. Phys. Lett. **114**, 114 (1985).
[17]M. E. Weber and P. B. Armentrout, J. Chem. Phys. **88**, 6898 (1988).
[18]M. E. Weber and P. B. Armentrout, J. Chem. Phys. **90**, 2213 (1989).
[19]M. E. Weber and P. B. Armentrout, J. Phys. Chem. **93**, 1596 (1989).
[20]K. M. Ervin and P. B. Armentrout, J. Chem. Phys. **84**, 6738 (1986).
[21]E. Teloy and D. Gerlich, Chem. Phys. **4**, 417 (1974).
[22]C. E. Moore, Natl. Bur. Stand. Natl. Stand. Ref. Data Ser. **34** (1970).
[23]P. M. Hierl, V. Pacak, and Z. Herman, J. Chem. Phys. **67**, 2678 (1977).
[24]K. E. Ervin and P. B. Armentrout, J. Chem. Phys. **86**, 6240 (1987).
[25]G. Gioumousis and D. P. Stevenson, J. Chem. Phys. **29**, 292 (1958).
[26]P. B. Armentrout, in *Structure/Reactivity and Thermochemistry of Ions*, edited by P. Ausloos and S. G. Lias (Reidel, Dordrecht, 1987), pp. 97–164.
[27]D. A. Dixon, J. Phys. Chem. **92**, 86 (1988).
[28]E. R. Lippencott and J. M. Stutman, J. Phys. Chem. **68**, 2926 (1964); E. R. Lippencott, G. Nagarajan, and J. M. Stutman, *ibid.* **70**, 78 (1966).
[29]E. W. Rothe and R. B. Bernstein, J. Chem. Phys. **31**, 1619 (1959).
[30]H. E. Watson and K. L. Ramaswamy, Proc. R. Soc. Ser. A **156**, 144 (1936).
[31]J. Müller, E. Poulain, O. Goscinski, and L. Karlsson, J. Chem. Phys. **72**, 2587 (1980).
[32]These values are the values obtained as described in Ref. 18.
[33]N. Aristov and P. B. Armentrout, J. Am. Chem. Soc. **108**, 1806 (1986); L. S. Sunderlin, N. Aristov, and P. B. Armentrout, *ibid.* **109**, 78 (1987).
[34]W. J. Chesnavich and M. T. Bowers, J. Phys. Chem. **83**, 900 (1979).
[35]B. H. Boo and P. B. Armentrout, J. Am. Chem. Soc. **109**, 3549 (1987).
[36]In most data sets, the CF^+ channel also exhibited an exothermic feature. However, this feature fell off steeply as $E^{-1.7 \pm 0.7}$ and the magnitude varied from 0.05 to 0.6 $Å^2$ at 0.1 eV. This irreproducibility suggests that this feature is an experimental artifact (and hence is not shown in Fig. 3) which we believe is due to nonreactive scattering of the reactant ions (Ref. 37). These scattered He^+ ions can be accelerated by the potential on the octopole rods and react upon further collision at anomalously high energies. Thus, reaction can be erroneously observed at low interaction energies, consistent with the behavior observed here. Only light reactant ions such as He^+ at low energies are subject to strong radial scattering and this effect. At energies higher than ~ 1 eV, this effect is not in evidence. Neither does it affect the low energy cross sections of reactions (4) and (5).
[37]K. M. Ervin and P. B Armentrout, J. Chem. Phys. **86**, 6240 (1987).
[38]Rate constants are derived from the cross sections by using the formula $k(E) = \sigma v$, where v is the relative velocity of the reactants. See Ref. 20.
[39]C. R. Brundle, M. B. Robin, and H. Basch, J. Chem. Phys. **53**, 2196 (1970).
[40]M. S. Banna and D. A. Shirley, Chem. Phys. Lett. **33**, 441 (1975).
[41](a) T. A. Walter, C. Lifshitz, W. A. Chupka, and J. Berkowitz, J. Chem. Phys. **51**, 3531 (1969); (b) G. Bieri, L. Åsbrink, and W. Von Niessen, J. Electron Spetrosc. Relat. Phenom. **23**, 281 (1981); (c) D. R. Lloyd and P. J. Roberts, *ibid.* **7**, 325 (1975); (d) W. E. Bull, B. P. Pullen, F. A. Grimm, W. E. Moddeman, G. K. Schwietzer, and T. A. Carlson, Inorg. Chem. **9**, 2474 (1970); (e) T. A. Carlson, A. Fahlman, W. A. Svensson, M. O. Krause, T. A. Whitley, F. A. Grimm, M. N. Piancastelli, and J. W. Taylor, J. Chem. Phys. **81**, 3828 (1984).
[42]J. F. M. Aarts, S. M. Mason, and R. P. Tuckett, Mol. Phys. **60**, 761 (1987).
[43]I. G. Simm, J. C. Danby, J. H. Eland, and P. I. Mansell, J. Chem. Soc. Faraday II **72**, 426 (1976).
[44]T. M. Mayer and R. A. Barker, J. Electrochem. Soc. **129**, 585 (1982).

Downloaded 11 Aug 2009 to 155.97.13.46. Redistribution subject to AIP license or copyright; see http://jcp.aip.org/jcp/copyright.jsp